Supporting Information

Inhibiting Polysulfides Shuttling by Dual-Functional Nanowires/Nanotubes Modified Layers for Highly Stable Lithium-Sulfur Batteries

Yizhou Wang,[a] Wenhui Liu,[a] Ruiqing Liu,[a] Peifeng Pan,[a] Liyao Suo,[a] Jun Chen,[a] Xiaomiao Feng,[a] Xizhang Wang,[b] Yanwen Ma,*[a] Wei Huang[a,c]*

a. Key Laboratory for Organic Electronics and Information Displays & Jiangsu Key Laboratory for Biosensors, Institute of Advanced Materials (IAM), Jiangsu National Synergetic Innovation Center for Advanced Materials (SICAM), Nanjing University of Posts & Telecommunications, 9 Wenyuan Road, Nanjing 210023, China. E-mail: iamywma@njupt.edu.cn, iamrqliu@njupt.edu.cn

b. Key Laboratory of Mesoscopic Chemistry of MOE, Collaborative Innovation Center of Chemistry for Life Sciences, School of Chemistry and Chemical Engineering, Jiangsu Provincial Lab for Nanotechnology, Nanjing Laizhang New Material Technology Co., Ltd., Nanjing University, Nanjing, 210023 China.

c. Shaanxi Institute of Flexible Electronics (SIFE), Northwestern Polytechnical University (NPU), Xi'an 710072, China.

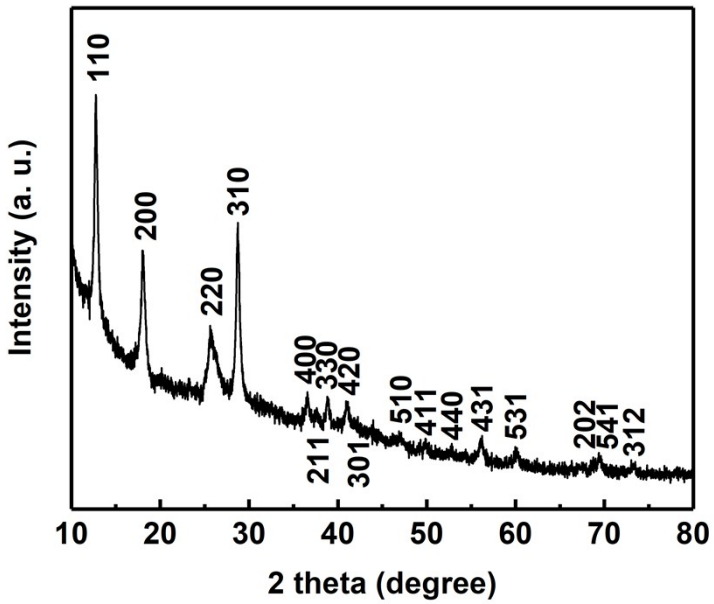

Figure S1. The XRD pattern of the synthesized MnO_2 nanowires.

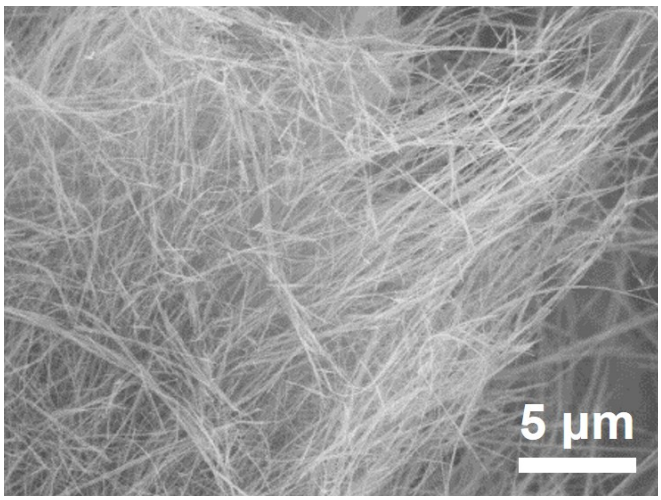

Figure S2. SEM images of the synthesized MnO_2 nanowires.

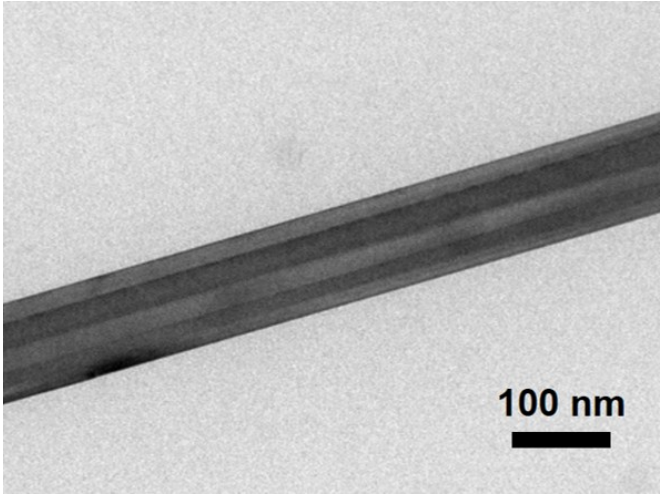

Figure S3. TEM images of the synthesized MnO_2 nanowires.

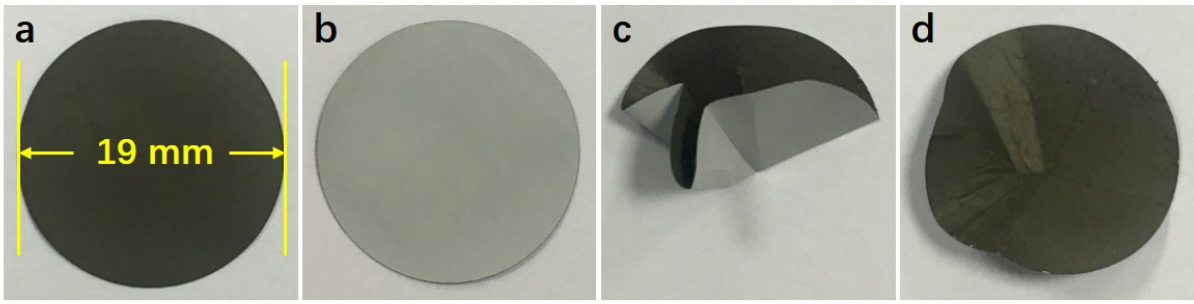

Figure S4. The optical photos of the MC-PP: (a) the modification side, (b) the back side, (c) the crumpled state, and (d) flat state after crumpling.

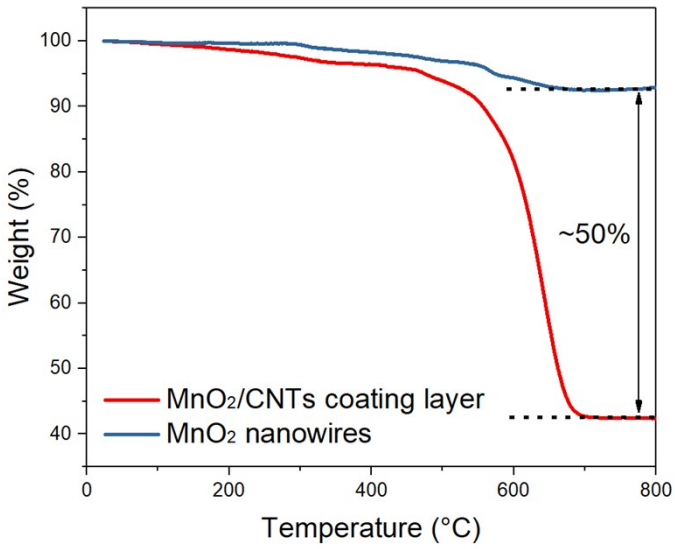

Figure S5. The TGA curves of MnO_2/CNTs coating layer and MnO_2 nanowires. The mass loss (about 8%) of MnO_2 nanowires could attribute to dehydration and the phase transition from MnO_2 to Mn_3O_4 and Mn_2O_3.[S1, S2] The mass loss during 500-700 ℃ mainly attributed to the loss of CNTs, and its ~50% mass ratio indicated the uniform distribution of MnO_2 and CNTs in the coating layer.

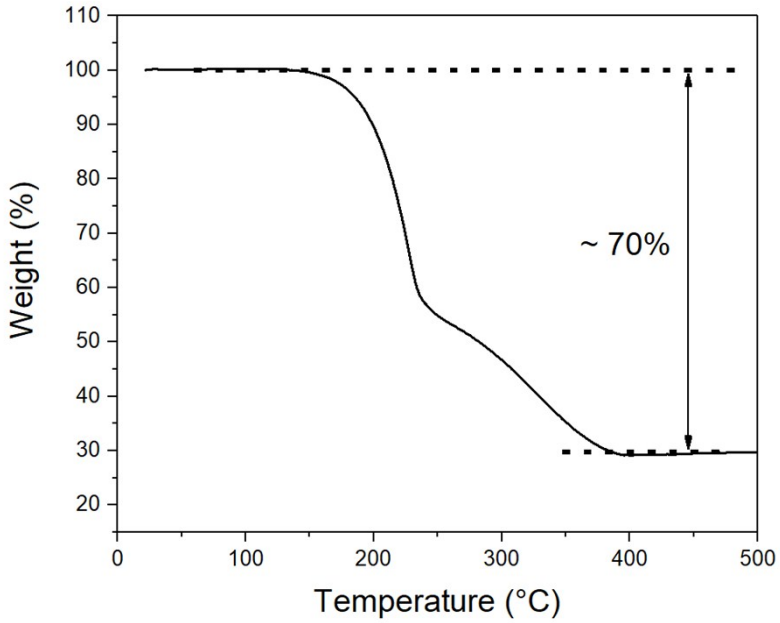

Figure S6. TGA of C/S composite under Ar flow. The two weight-loss steps could be due to the losses of sulfur at surface and in the pores of porous carbon, respectively.[S3]

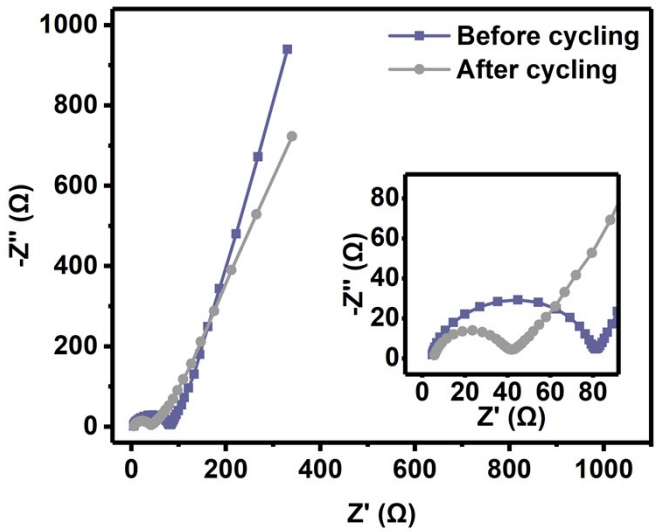

Figure S7. Nyquist plots of Li-S battery using MC-PP before and after cycling.

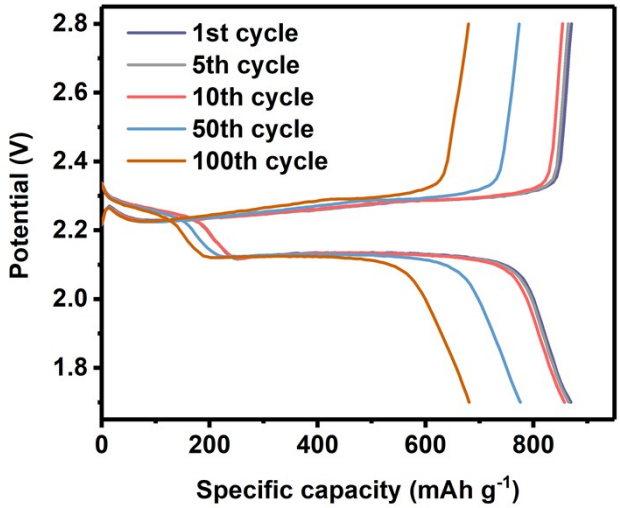

Figure S8. The typical voltage profiles of Li-S battery using MC-PP at 0.5 C at different cycles.

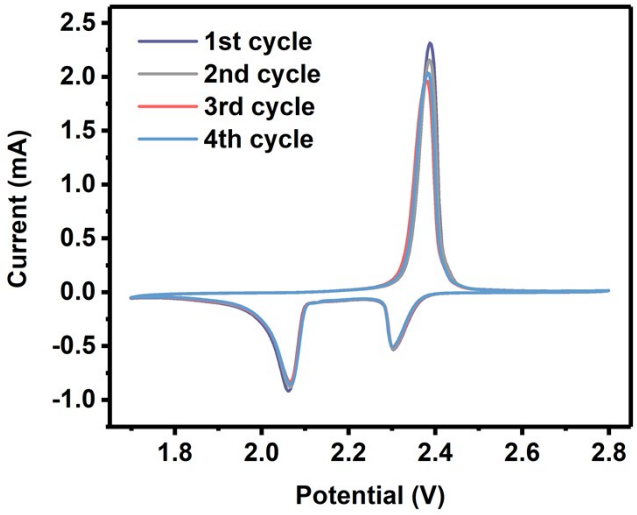

Figure S9. CV curves of Li-S batteries using MC-PP at a scan rate of 0.1 mV s^{-1} at different cycles.

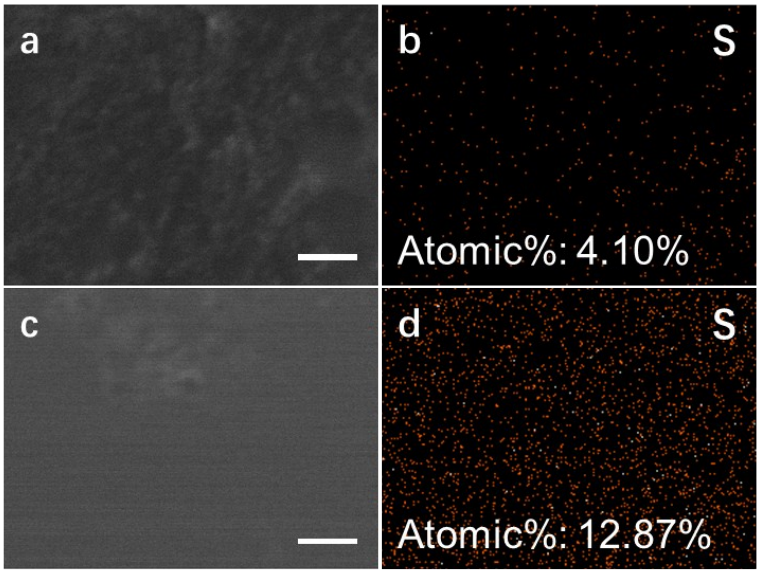

Figure S10. SEM image and EDS mapping (sulfur) of lithium metal anode after 100 cycles at 1 C with (a, b) MC-PP and (c, d) Bare PP.

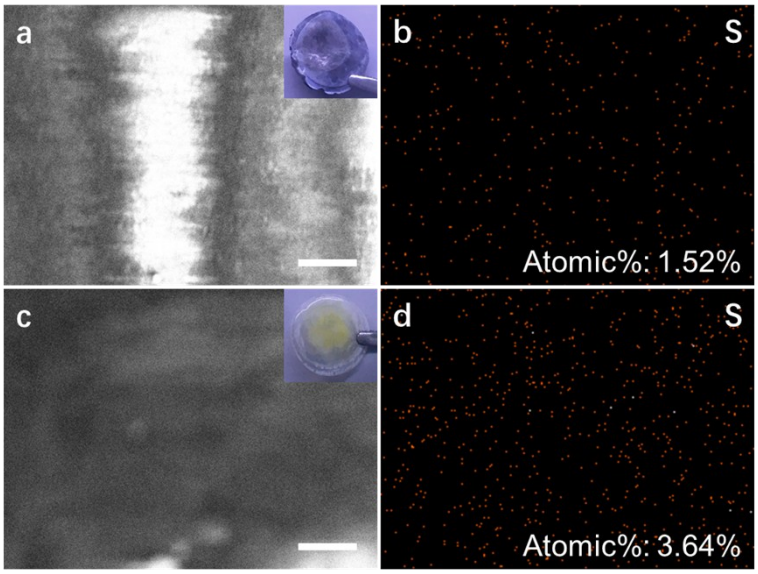

Figure S11. SEM image and EDS mapping (sulfur) of separators (anode side) after 100 cycles at 1 C with (a, b) MC-PP and (c, d) Bare PP. The insets are the digital photos of separators at anode side.

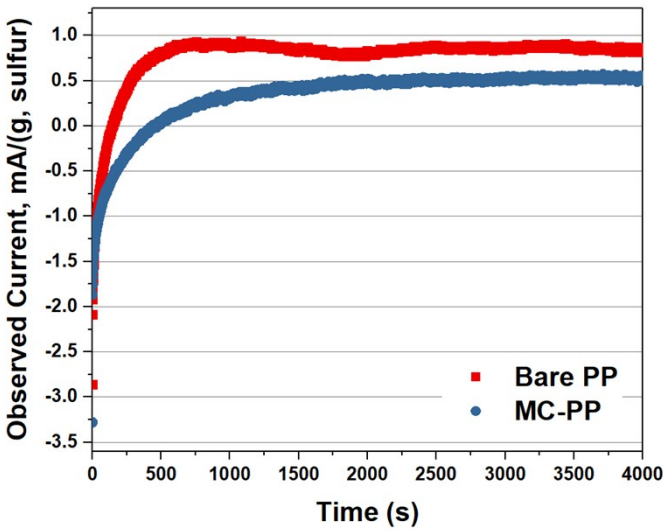

Figure S12. Shuttle currents of batteries with Bare PP and MC-PP. To conduct the measurement of shuttle current, first the battery was activated for 3 cycles and was charged to only 2.4 V in the last activation cycle, then the battery was rested at open circuit for 10 minutes and reach a stable potential. After that, a current was applied to the battery to keep the stable potential. The observed current would reach a stable value finally, and this value was the shuttle current of this battery.[S4]

References

[S1] A. M. Hashema, H. M. Abuzeida, K. Nikolowski, H. Ehrenberg, *J. Alloys Compd.*, 2010, **497**, 300.
[S2] R. K. Sharma, H.-S. Oh, Y.-G. Shul, H. Kim, *Physica B*, 2008, **403**, 1763.
[S3] J. Yang, J. Xie, X. Zhou, Y. Zou, J. Tang, S. Wang, F. Chen, L. Wang, *J. Phys. Chem. C*, 2014, **118**, 1800.
[S4] D. Moy, A. Manivannan, S. R. Narayanan, *J. Electrochem. Soc.*, 2015, **162**, A1.